Slip and Heat Transfer Effects on Peristaltic Motion of a Carreau Fluid in an Asymmetric Channel

Tasawar Hayat[a,b], Najma Saleem[a], and Awatif A. Hendi[c]

[a] Department of Mathematics, Quaid-i-Azam University, Islamabad 44000, Pakistan
[b] Department of Mathematics, College of Science, King Saud University, P. O. Box 2455, Riyadh 11451, Saudia Arabia
[c] Department of Physics, Faculty of Science, P.O. Box 1846, Riyadh 11321, Saudi Arabia

Reprint requests to T. H.; E-mail: pensy_t@yahoo.com

Z. Naturforsch. **65a,** 1121 – 1127 (2010); received November 20, 2009 / revised April 23, 2010

An analysis has been carried out for peristaltic flow and heat transfer of a Carreau fluid in an asymmetric channel with slip effect. The governing problem is solved under long wavelength approximation. The variations of pertinent dimensionless parameters on temperature are discussed. Pumping and trapping phenomena are studied.

Key words: Heat Transfer; Slip Condition; Carreau Fluid; Asymmetric Channel.

1. Introduction

Peristaltic transport of a fluid in channels has been a subject of great interest for the last four decades. Such interest is motivated by several applications of peristaltic flows in engineering and industry. In animals and human bodies, the physiological fluids pumped by the muscular oscillations which correspond to peristaltic activity. In particular, the flow of blood through arteries and veins, the flow of urine through ureter, the motion of chyme in the gastrointestinal tract, transport of food bolus through alimentary canal, the movement of some worms and many others are examples of peristaltic motion. Roller and finger pumps also work in accordance with this motion. After the pioneering work of Latham [1], many investigators have studied the peristaltic motion under different assumptions [2 – 15].

The heat transfer analysis is important in processes of hemodialysis and oxygenation. It is noted from the existing studies that much has not been said about the peristaltic motion with heat transfer. Few studies describing heat transfer effects on the peristaltic motion can be mentioned by the investigations [16 – 22]. Note that analysis of peristaltic motion with heat transfer is of considerable interest in various physical situations. Furthermore, the slip effects in elastic fluids are encountered under a long tangential direction [23 – 26]. Such effects frequently appear in non-Newtonian fluids, flow of blood through capillary vessels, concentrated polymer solutions, and molten polymers.

This paper concentrates on the simultaneous effects of heat transfer and slip on peristaltic motion in an asymmetric channel. The mathematical formulation is based upon the constitutive equations of a Carreau fluid. Slip condition in terms of shear stress is considered. The solution of the resulting problem is presented after utilizing long wavelength approximation. Results of stream function, pressure gradient, and temperature are developed. Pumping, trapping, and frictional forces are discussed in detail.

2. Mathematical Analysis

We consider an incompressible Carreau fluid in an asymmetric channel of width $d_1 + d_2$. The flow here is due to propagation of waves on the channel walls. The expressions of such waves are

$$\begin{aligned} Y &= h_1'(X,Y,t) \\ &= d_1 + a_1 \cos\left(\frac{2\pi}{\lambda}(X - c\acute{t})\right) \quad \text{upper wall,} \\ Y &= h_2'(X,Y,t) \\ &= -d_2 - b_1 \cos\left(\frac{2\pi}{\lambda}(X - c\acute{t}) + \phi\right) \quad \text{lower wall,} \end{aligned} \tag{1}$$

in which a_1, b_1 are the wave amplitudes, λ is the wavelength, $\acute{t}$ is the time, $d_1 + d_2$ is the channel width, and $\phi(0 \le \phi \le \pi)$ is the phase difference. Note that asymmetry in the channel is induced because of different amplitudes and phases. For $\phi = 0$ there is a symmetric

channel with waves in phase, and $\phi = \pi$ correponds to the case when waves are out of phase. Also a_1, b_1, d_1, and d_2 satisfy the condition

$$a_1^2 + b_1^2 + 2a_1 b_1 \cos\phi \le (d_1 + d_2)^2.$$

The transformations in the laboratory (X', Y') and wave (x', y') frames are

$$\begin{aligned} &x' = X' - ct', \quad y' = Y', \\ &u'(x', y') = U' - c, \quad v'(x', y') = V', \end{aligned} \tag{2}$$

where (U', V') and (u', v') are the respective velocities in the laboratory and wave frames.

An extra stress tensor $\bar{\boldsymbol{\tau}}$ in a Carreau fluid [27–31] is given by

$$\bar{\boldsymbol{\tau}} = -\left(\eta_0 \left(1 + \left(\Gamma\bar{\dot{\gamma}}\right)^2\right)^{\frac{n-1}{2}}\right)\bar{\dot{\gamma}}, \tag{3}$$

$$\bar{\dot{\gamma}} = \sqrt{\frac{1}{2}\sum_i\sum_j \bar{\dot{\gamma}}_{ij}\bar{\dot{\gamma}}_{ji}} = \sqrt{\frac{1}{2}\pi}, \tag{4}$$

in which η_0 is the zero shear-rate viscosity, Γ the time constant, n the dimensionless power law index, π the second invariant of strain-rate tensor, and infinite shear stress viscosity is absent. Note that for $n = 1$ or $\Gamma = 0$ (3) corresponds to the case of a Newtonian fluid.

The velocity field is defined by the following expression:

$$\bar{\mathbf{V}}' = (u', v', 0). \tag{5}$$

On setting

$$\begin{aligned} &x = \frac{2\pi x'}{\lambda}, \quad y = \frac{y'}{d_1}, \quad u = \frac{u'}{c}, \quad v = \frac{v'}{c}, \\ &t = \frac{2\pi t' c}{\lambda}, \quad p = \frac{2\pi d_1^2 p'}{c\lambda\mu}, \quad Re = \frac{\rho c a}{\mu} \\ &\tau = \frac{d_1\tau'}{\mu c}, \quad h_1 = \frac{h_1'}{d_1}, \quad h_2 = \frac{h_2'}{d_1}, \quad \Psi = \frac{\Psi'}{c d_1}, \\ &\delta = \frac{2\pi d_1}{\lambda}, \quad d = \frac{d_2}{d_1}, \quad a = \frac{a_1}{d_1}, \quad b = \frac{a_2}{d_1}, \\ &\theta' = \frac{T - T_0}{T_1 - T_0}, \quad Pr = \frac{\rho\nu C_p}{\kappa}, \quad Ec = \frac{c^2}{C_p\left(T_1 - T_0\right)}, \\ &u = \frac{\partial\Psi}{\partial y}, \quad v = -\delta\frac{\partial\Psi}{\partial x}, \quad Br = Ec\,Pr, \end{aligned} \tag{6}$$

the continuity equation is identically satisfied and momentum and energy equations give

$$\begin{aligned} &Re\delta\left\{\left(\frac{\partial\Psi}{\partial y}\frac{\partial}{\partial x} - \frac{\partial\Psi}{\partial x}\frac{\partial}{\partial y}\right)\frac{\partial\Psi}{\partial y}\right\} = \\ &\quad -\frac{\partial p}{\partial x} - \delta\frac{\partial\tau_{xx}}{\partial x} - \frac{\partial\tau_{xy}}{\partial y}, \end{aligned} \tag{7}$$

$$\begin{aligned} &-Re\delta^3\left\{\left(\frac{\partial\Psi}{\partial y}\frac{\partial}{\partial x} - \frac{\partial\Psi}{\partial x}\frac{\partial}{\partial y}\right)\frac{\partial\Psi}{\partial x}\right\} = \\ &\quad -\frac{\partial p}{\partial y} - \delta^2\frac{\partial\tau_{xy}}{\partial x} - \delta\frac{\partial\tau_{yy}}{\partial x}, \end{aligned} \tag{8}$$

$$\begin{aligned} &\frac{\partial^2\theta'}{\partial y^2} + Br\left\{1 + \frac{(n-1)}{2}We^2\dot{\gamma}^2\right\} \\ &\quad \cdot\left(\frac{\partial^2\Psi}{\partial y^2} - \delta^2\frac{\partial^2\Psi}{\partial x^2}\right)\frac{\partial^2\Psi}{\partial y^2} = 0, \end{aligned} \tag{9}$$

hence,

$$\tau_{xx} = -2\left[1 + \frac{(n-1)}{2}We^2\dot{\gamma}^2\right]\frac{\partial^2\Psi}{\partial x\partial y}, \tag{10}$$

$$\begin{aligned} \tau_{xy} = &-\left[1 + \frac{(n-1)}{2}We^2\dot{\gamma}^2\right] \\ &\cdot\left(\frac{\partial^2\Psi}{\partial y^2} - \delta^2\frac{\partial^2\Psi}{\partial x^2}\right), \end{aligned} \tag{11}$$

$$\tau_{yy} = 2\delta\left[1 + \frac{(n-1)}{2}We^2\dot{\gamma}^2\right]\frac{\partial^2\Psi}{\partial x\partial y}, \tag{12}$$

$$\begin{aligned} \dot{\gamma} = &\left[2\delta^2\left(\frac{\partial^2\Psi}{\partial x\partial y}\right)^2 + \left(\frac{\partial^2\Psi}{\partial y^2} - \delta^2\frac{\partial^2\Psi}{\partial x^2}\right)^2\right. \\ &\left. + 2\delta^2\left(\frac{\partial^2\Psi}{\partial x\partial y}\right)^2\right]^{\frac{1}{2}}, \end{aligned} \tag{13}$$

where δ is the wave number, p the pressure, We the Wessinberg number, Re the Reynolds number, Pr the Prandtl number, Ec the Eckert number, and Br the Brinkman number.

Using long wavelength [32–36] and low Reynolds number approximations, (7) to (9) can be written as

$$\frac{\partial p}{\partial x} = \frac{\partial}{\partial y}\left[\left\{1 + \frac{(n-1)}{2}We^2\left(\frac{\partial^2\Psi}{\partial y^2}\right)^2\right\}\frac{\partial^2\Psi}{\partial y^2}\right], \tag{14}$$

$$\frac{\partial p}{\partial y} = 0, \tag{15}$$

$$\frac{\partial^2\theta'}{\partial y^2}+Br\left[\left\{1+\frac{(n-1)}{2}\cdot We^2\left(\frac{\partial^2\Psi}{\partial y^2}\right)^2\right\}\left(\frac{\partial^2\Psi}{\partial y^2}\right)^2\right]=0, \tag{16}$$

where (15) shows that $p\neq p(y)$ and, hence, $p=p(x)$.

From (14) and (15), we get

$$\frac{\partial^2}{\partial y^2}\left[\left\{1+\frac{(n-1)}{2}We^2\left(\frac{\partial^2\Psi}{\partial y^2}\right)^2\right\}\frac{\partial^2\Psi}{\partial y^2}\right]=0. \tag{17}$$

The dimensionless boundary conditions are [5]

$$\begin{aligned}&\Psi=\frac{F}{2},\quad \frac{\partial\Psi}{\partial y}=\beta\tau_{xy}-1,\\ &\theta'=0\ \text{ at }\ y=h_1=1+a\cos 2\pi x,\\ &\Psi=-\frac{F}{2},\quad \frac{\partial\Psi}{\partial y}=-\beta\tau_{xy}-1,\\ &\theta'=1\ \text{ at }\ y=h_2=-d-b\cos(2\pi x+\phi),\end{aligned} \tag{18}$$

where $\beta=\left(\frac{L}{d_1}\right)$ is the dimensionless slip parameter, L is the dimensional slip parameter, and h_1 and h_2 are the dimensional form of the peristaltic walls. The boundary conditions (18) after utilizing the long wavelength approximation reduce to

$$\begin{aligned}&\Psi=\frac{F}{2},\\ &\frac{\partial\Psi}{\partial y}=-\beta\left\{\left(\frac{\partial^2\Psi}{\partial y^2}\right)+\frac{(n-1)}{2}We^2\left(\frac{\partial^2\Psi}{\partial y^2}\right)^3\right\}-1,\\ &\theta'=0\ \text{ at }\ y=h_1=1+a\cos 2\pi x,\quad \Psi=-\frac{F}{2},\\ &\frac{\partial\Psi}{\partial y}=\beta\left\{\left(\frac{\partial^2\Psi}{\partial y^2}\right)+\frac{(n-1)}{2}We^2\left(\frac{\partial^2\Psi}{\partial y^2}\right)^3\right\}-1,\\ &\theta'=1\ \text{ at }\ y=h_2=-d-b\cos(2\pi x+\phi).\end{aligned} \tag{19}$$

The dimensionless mean flow rates in laboratory (θ) and wave (F) frames are

$$\theta=F+d+1, \tag{20}$$

$$F=\int_{h_2(x)}^{h_1(x)}\frac{\partial\Psi}{\partial y}\mathrm{d}y=\Psi(h_1(x))-\Psi(h_2(x)), \tag{21}$$

and pressure rise is

$$\Delta p_\lambda=\int_0^{2\pi}\left(\frac{\mathrm{d}p}{\mathrm{d}x}\right)\mathrm{d}x. \tag{22}$$

For small We we write

$$\Psi=\Psi_0+We^2\Psi_1+O(We^4), \tag{23}$$

$$F=F_0+We^2F_1+O(We^4), \tag{24}$$

$$p=p_0+We^2p_1+O(We^4). \tag{25}$$

Upon making use of above equations into (14) and (16)–(18) and then solving the resulting systems we have

$$\begin{aligned}\Psi=&\frac{1}{10(h_1-h_2)^6(6\beta+h_1-h_2)^4}((2y-h_1-h_2)\\ &\cdot(-10(y-h_1)(y-h_2)(h_1-h_2)^5+(6\beta+h_1-h_2)^3\\ &+We^2(-216F^3(-1+n)(y-h_1)(y-h_2)(-6y^2\beta\\ &+h_1(-y(y-6\beta)+(y+2\beta)h_1)+(y(y+6\beta)\\ &-h_1(10\beta+h_1)h_2+(-y+2\beta+h_1)h_2^2)\\ &+648F^2(-1+n)(-y+h_1)(y-h_2)(h_1-h_2)(-6y^2\beta\\ &+h_1(-y(y-6\beta)+(y+2\beta)h_1)+(y(y+6\beta)\\ &-h_1(10\beta+h_1))h_2+(-y+2\beta+h_1)h_2^2)\\ &+648F(-1+n)(-y+h_1)(y-h_2)(h_1-h_2)^2(-6y^2\beta\\ &+h_1(-y(y-6\beta)+(y+2\beta)h_1)+(y(y(y+6\beta)\\ &-h_1(10\beta+h_1))h_2+(-y+2\beta+h_1)h_2^2)\\ &+(h_1-h_2)^3(1296(-1+n)y^4\beta+216h_1^3(-1+n)\\ &\cdot(y-h_1)(y+2\beta-h_2)+216(-1+n)yh_2(-y^2\\ &\cdot(y+12\beta)+2y(y+2\beta)h_2-(y-2\beta)h_2^2\\ &+216(-1+n)yh_1(y^3(y-12\beta)+28y^2\beta h_2\\ &-y(3y+14\beta)h_2^2+(y-\beta)h_2^3)-216(-1+n)h_1^2\\ &\cdot(2y(y-2\beta)-h_2(y-10\beta-h_2))))))),\end{aligned} \tag{26}$$

$$\begin{aligned}\frac{\mathrm{d}p}{\mathrm{d}x}=&\frac{1}{5(h_1-h_2)^4(6\beta+h_1-h_2)^4}(12(540F^2(-1+n)\\ &\cdot We^2\beta+(54F(-1+n)We^2(F+20\beta)\\ &+(108(F(-1+n)We^2+5(-1+n)We^2\beta+10\beta^3)\\ &+(54(-1+n)We^2+540\beta^2+5(h_1-h_2)\\ &\cdot(18\beta+h_1-h_2))(h_1-h_2))(h_1-h_2))(h_1-h_2))\\ &\cdot(F+h_1-h_2)).\end{aligned} \tag{27}$$

3. Results and Discussion

The main emphasis in this section is given to analyze the phenomena of pumping, trapping, and frictional forces. First, the pumping characteristic against pressure rise per wavelength Δp_λ is discussed. Δp_λ is denoted by p_0 at zero volume flow rate θ. When $\Delta p_\lambda > p_0$ then we have negative flux. The regions $\Delta p_\lambda = 0$, $\Delta p_\lambda > 0$, and $\Delta p_\lambda < 0$ correspond to free pumping, peristaltic pumping, and copumping regions, respectively. In order to discuss the pumping phenomenon, numerical integration is made and results are plotted. The effects of slip parameter β on Δp_λ is given in Figure 1. It shows that the peristaltic pumping rate increases by increasing β. The results of no-slip condition can be taken by choosing $\beta = 0$.

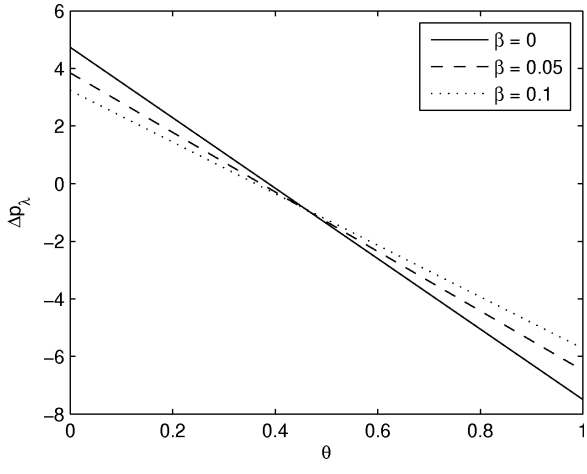

Fig. 1. Plot showing Δp_λ versus y. Here $n = 0.398$, $We = 0.01$, $a = b = 0.4$, $d = 1.1$, and $\phi = \frac{\pi}{6}$.

Another interesting phenomenon of peristalsis is trapping. In the wave frame the streamlines are plotted for an asymmetric channel. To see the effects of physical parameters of interest we have prepared Figures 2 and 3. Figure 2 describes the variations of the slip parameter β on trapping. This figure shows that with an increase of β, the upper bolus is going to expand and the lower one is going to squeeze. The dimensionless flow rate θ is displayed in Figure 3. Here the size of the upper bolus increases and of the lower bolus decreases when θ is increased.

The temperature θ' for different Brinkman number Br, phase difference ϕ, and volume flow rate θ is sketched in Figures 4–6. Figure 4 depicts the effects of Br on the temperature. In this figure temperature increases when Br increases. The temperature profile is almost parabolic. Figure 5 describes the influence of ϕ on the temperature. Clearly temperature decreases when ϕ increases. It is noted that temperature increases much in symmetric channel. The effects of θ on the temperature θ' is displayed in Figure 6. It is noted that the temperature increases with an increase in θ and the temperature profile looks parabolic.

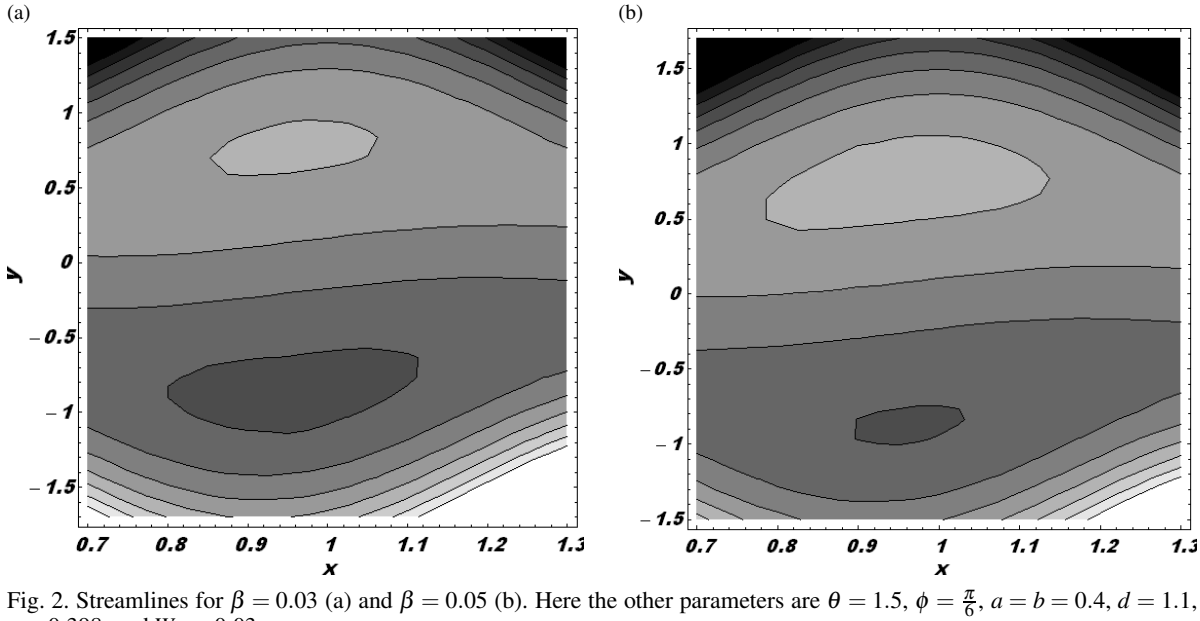

Fig. 2. Streamlines for $\beta = 0.03$ (a) and $\beta = 0.05$ (b). Here the other parameters are $\theta = 1.5$, $\phi = \frac{\pi}{6}$, $a = b = 0.4$, $d = 1.1$, $n = 0.398$, and $We = 0.03$.

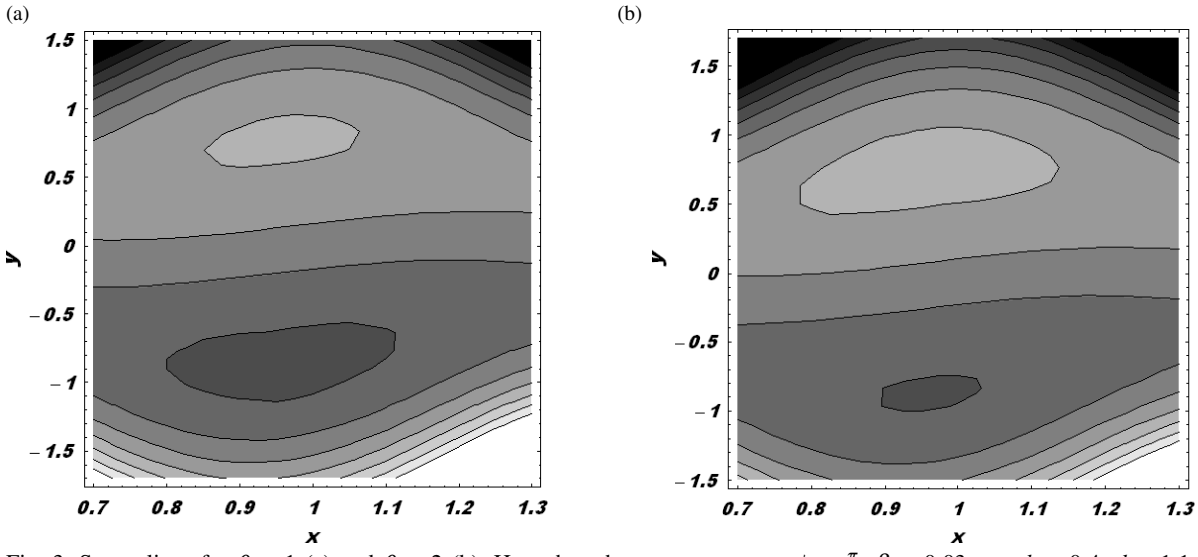

Fig. 3. Streamlines for $\theta = 1$ (a) and $\theta = 2$ (b). Here the other parameters are $\phi = \frac{\pi}{6}$, $\beta = 0.03$, $a = b = 0.4$, $d = 1.1$, $n = 0.398$, and $We = 0.03$.

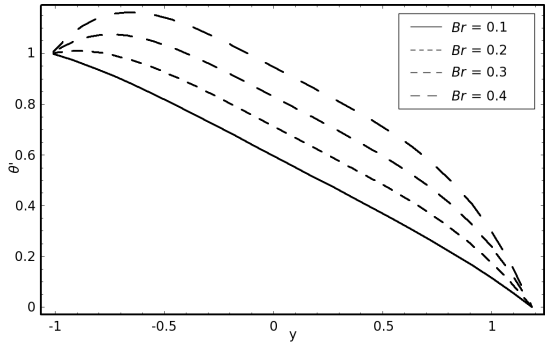

Fig. 4. Effects of Brinkman number Br on the temperature distribution. Here the other parameters are $a = 0.6$, $b = 0.3$, $d = 1.1$, $n = 0.398$, $We = 0.01$, $\beta = 0.03$, $\theta = 2$, $\phi = \frac{\pi}{6}$, and $x = 0.1$.

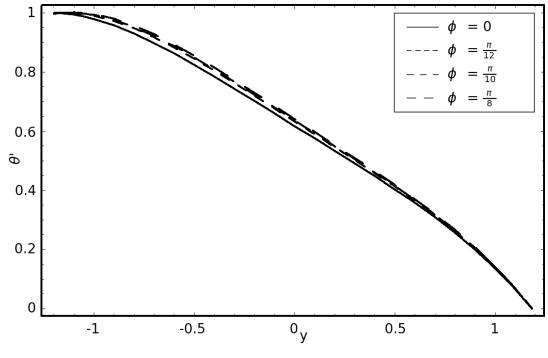

Fig. 5. Effects of phase difference ϕ on the temperature distribution. Here the other parameters are $a = 0.6$, $b = 0.3$, $d = 1.1$, $n = 0.398$, $We = 0.01$, $\beta = 0.03$, $\theta = 2$, $Br = 0.2$, and $x = 0.1$.

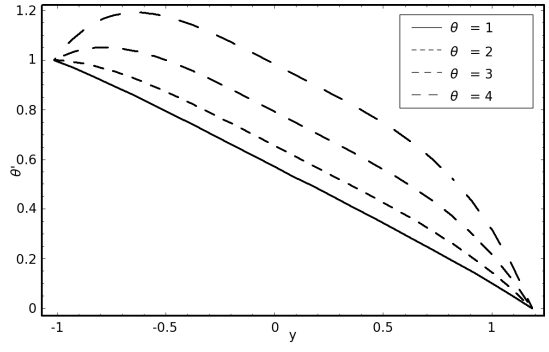

Fig. 6. Effects of volume flow rate θ on the temperature distribution. Here the other parameters are $a = 0.6$, $b = 0.3$, $d = 1.1$, $n = 0.398$, $We = 0.01$, $\beta = 0.03$, $\phi = \frac{\pi}{6}$, $Br = 0.2$, and $x = 0.1$.

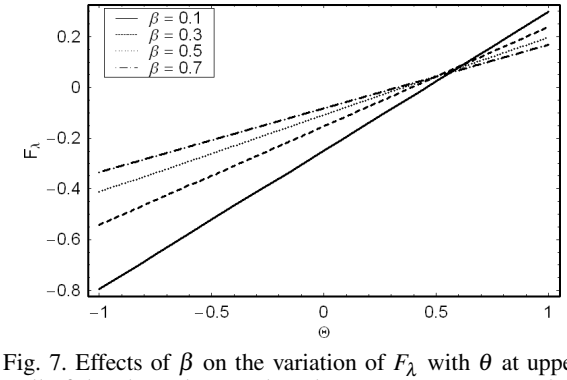

Fig. 7. Effects of β on the variation of F_λ with θ at upper wall of the channel. Here the other parameters are $a = 0.7$, $b = 1.2$, $d = 2$, $n = 0.398$, $We = 0.01$, and $\phi = \frac{3\pi}{2}$.

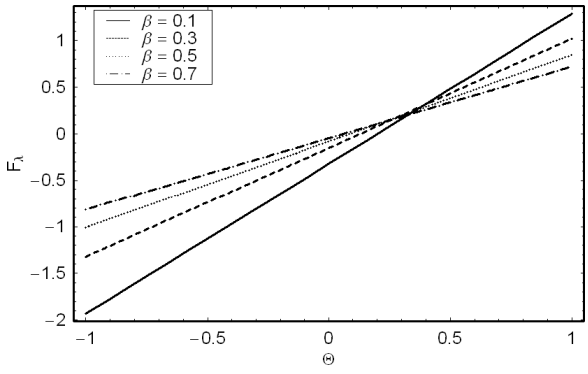

Fig. 8. Effects of β on the variation of F_λ with θ at lower wall of the channel. Here the other parameters are $a = 0.7$, $b = 1.2$, $d = 2$, $n = 0.398$, $We = 0.01$, and $\phi = \frac{3\pi}{2}$.

Figures 7 and 8 explain the frictional forces F_λ for various values of the slip parameter β at the channel walls. The frictional forces versus mean flow rate θ at the upper wall of the channel can be seen in Figure 7. In this figure there is a critical value of θ ($0 < \theta < 0.5$) for which F_λ resists the flow along the channel wall. Above (below) this critical point F_λ decreases (increases) for large values of β. Figure 8 is plotted for the variation of β on the lower wall of the channel and its behaviour is quite similar to that of Figure 7.

4. Concluding Remarks

The effect of slip and heat transfer on peristalsis of a Carreau fluid have been carried out under long wavelength and low Reynolds number assumptions. The series solutions for pressure gradient, stream function, and temperature distribution are derived when the Wessinberg number is small. It is concluded that the size of the upper trapped bolus increases and that of lower one decreases for large values of slip parameter and dimensionless volume flow rate. Further, temperature is an increasing function of Brinkman number and dimensionless volume flow rate. However, the temperature decreases by increasing phase difference.

Acknowledgements

We are grateful to the reviewers for their valuable suggestions. The first author (as a visiting Professor) is thankful to the King Saud University for the support (KSU-VPP-103). The financial support under URF of Quaid-i-Azam University is also acknowledged.

[1] T. W. Latham, Fluid motion in a peristaltic pump, MIT, Cambridge, MA 1966.
[2] T. Hayat, M. U. Qureshi, and N. Ali, Phys. Lett. A **372**, 2653 (2008).
[3] N. Ali, Q. Hussain, T. Hayat, and S. Asghar, Phys. Lett. A **372**, 1477 (2008).
[4] T. Hayat, F. M. Mahomed, and S. Asghar, Nonlinear Dyn. **40**, 375 (2005).
[5] M. Mishra and A. R. Rao, Z. Angew. Math. Phys. **54**, 532 (2003).
[6] G. Radhakrishnamacharya, Rheol. Acta **21**, 30 (1982).
[7] A. H. Shapiro, M. Y. Jaffrin, and S. L. Weinberg, J. Fluid Mech. **37**, 799 (1969).
[8] M. Kothandapani and S. Srinivas, Int. J. Nonlinear Mech. **43**, 915 (2008).
[9] M. Kothandapani and S. Srinivas, Phys. Lett. A **372**, 915 (2008).
[10] Kh. S. Mekheimer and Y. Abd elmaboud, Physica A: Stat. Mech. Appl. **387**, 2403 (2008).
[11] Kh. S. Mekheimer, Appl. Math. Comput. **153**, 763 (2004).
[12] T. Hayat and N. Ali, Physica A **371**, 188 (2006).
[13] T. Hayat, N. Ali, and S. Asghar, Appl. Math. Comput. **186**, 309 (2007).
[14] T. Hayat, N. Ali, and Z. Abbas, Phys. Lett. A **370**, 331 (2007).
[15] T. Hayat and N. Ali, Math. Comput. Modell. **48**, 721 (2008).
[16] Kh. S. Mekheimer and Y. Abd elmaboud, Phys. Lett. A **372**, 1657 (2008).
[17] M. Kothandapani and S. Srinivas, Phys. Lett A **372**, 4586 (2008).
[18] V. Vajravelu, G. Radhakrishnamacharya, and V. Radhakrishnamurty, Int. J. Nonlinear Mech. **42**, 754 (2007).
[19] M. Kothandapani and S. Srinivas, Phys. Lett A **372**, 4586 (2008).
[20] K. Vajravelu, G. Radhakrishnamacharya, and V. Radhakrishnamurty, Int. J. Nonlinear Mech. **42**, 754 (2007).
[21] S. Nadeem and N. S. Akbar, Commun. Nonlinear Sci. Numer. Simul. **14**, 4100 (2009).
[22] T. Hayat, M. Umar Qureshi, and Q. Hussain, Appl. Math. Modell. **33**, 1862 (2009).
[23] R. Ellahi, Commun. Nonlinear Sci. Numer. Simul. **14**, 1377 (2009).
[24] R. Ellahi, T. Hayat, F. M. Mahomed, and S. Asghar, Nonlinear Analysis Series B: Real World Appl. **1**, 139 (2010).
[25] R. Ellahi, T. Hayat, F. M. Mahomed, and A. Zeeshan, Commun. Nonlinear Sci. Numer. Simul. **15**, 322 (2010).

[26] T. Hayat, R. Ellahi, and S. Asghar, Int. J. Appl. Mech. Eng. **13**, 101 (2008).
[27] A. Abd El Naby, A. E. M. El Misiery, and M. F. Abd El Kareem, Physica A **343**, 1 (2004).
[28] N. Ali and T. Hayat, Appl. Math. Comput. **193**, 535 (2007).
[29] T. Hayat, N. Saleem, and N. Ali, Commun. Nonlinear Sci. Numer. Simul. **15**, 2407 (2010).
[30] J. P. Hsu, C. Y. Chen, L. H. Yeh, and S. Tseng, Colloids and Surfaces B: Biointerfaces **69**, 8 (2009).
[31] A. Abd El Naby, A. E. M. El Misery, and M. F. Abd El Kareem, Physica A: Stat. Mech. Appl. **367**, 79 (2006).
[32] A. H. Shapiro, M. Y. Jaffrin, and S. L. Weinberg, J. Fluid Mech. **37**, 799 (1969).
[33] G. Radhakrishnamacharya, Rheol. Acta **21**, 30 (1982).
[34] S. Usha and A. R. Rao, Trans. ASME J. Biomech. Eng. **199**, 483 (1997).
[35] T. Hayat, F. M. Mahomed, and S. Asghar, Nonlinear Dyn. **40**, 375 (2005).
[36] N. Ali, Y. Wang, T. Hayat, and M. Oberlack, Biorheol. **45**, 611 (2008).